1997MNRAS.290..231S

Mon. Not. R. Astron. Soc. **290,** 231–244 (1997)

The nature of the optical continuum in NGC 5128 (Centaurus A)

Thaisa Storchi-Bergmann,[1⋆] Eduardo Bica,[1] Anne L. Kinney[2⋆] and Charles Bonatto[1]
[1]*Departamento de Astronomia, IF-UFRGS, CP 15051, CEP 91501-970, Porto Alegre, RS, Brazil*
[2]*Space Telescope Science Institute, 3700 San Martin Drive, Baltimore, MD 21218, USA*

Accepted 1997 March 21. Received 1997 January 7; in original form 1996 September 16

ABSTRACT

We present long-slit observations of NGC 5128 in the range λλ3200–9800 Å, covering the nucleus and dust lane across the east–west direction, up to ≈2.2 kpc from the nucleus. The reddening-corrected continua and absorption features, when compared with those typical of a bulge stellar population, show that all locations within 1.8 kpc from the nucleus present a diluting continuum in the blue. We investigate the nature of the continuum by constructing models which consider the possible contribution of a metal-rich old bulge, a blue stellar population and a power-law component from scattered nuclear light. By matching the equivalent widths of the absorption lines, continuum slopes and 4000-Å break in our spectra with those of the models, we find that: (i) at all locations the dominant contribution (in flux at 5870 Å) comes from a metal-rich old bulge; (ii) the diluting continuum is well reproduced by a power-law component alone in the two locations at the borders of the dusty disc; (iii) in the locations closer to the nucleus along the dust lane, the diluting continuum can be represented by the spectra of blue stellar populations subject to different amounts of reddening, denoting the presence of recent star formation at different depths along the dust lane; nevertheless, some contribution of a power law from scattered nuclear light to the blue component cannot be ruled out by our data. From the optical continuum distributions, we conclude that the regions within a projected distance $d < 0.3$ kpc from the nucleus are affected by a large reddening, with $A_V \approx 3$ mag, whereas at $d \approx 1.8$ kpc, A_V decreases to ≈0.6 mag. Gas properties were obtained from the stellar population-subtracted emission lines, confirming previous findings that several emitting regions have H II region characteristics, consistent with the derived blue stellar population contribution. However, near-infrared lines also indicate some contribution from shocks. The nucleus and locations between 1.0 and 1.5 kpc to the west have LINER-like spectra. All the above properties can be understood within a scenario in which a dusty star-forming disc is interacting with the giant elliptical radio galaxy. For the nucleus we are able to match with the same aperture, our visible–near-infrared spectrum with that obtained by the *International Ultraviolet Explorer* (*IUE*). A reddening analysis of this spectrum shows that at different wavelength ranges we are probing different depths: while in the near-infrared $A_V \approx 3.0$ mag and the stellar population is dominated by the bulge, in the ultraviolet it appears to be dominated by that of a young disc with $A_V \approx 0.9$ mag.

Key words: dust, extinction – galaxies: active – galaxies: individual: NGC 5128 (Cen A) – galaxies: stellar content.

1 INTRODUCTION

The nature of the ultraviolet/optical continuum in radio galaxies has been a matter of some controversy in the literature, mainly in association with the 'alignment effect' (McCarthy et al. 1987; Chambers, Miley & van Breugel 1987): it was found that this continuum in high-redshift radio galaxies presents an ultraviolet excess, and is closely aligned with the axes of the large-scale radio structures. The two most favoured interpretations for this effect are the triggering of star formation by the passage of a radio jet through the interstellar medium, and light scattered from an anisotropic radiation field of a hidden active galactic nucleus (AGN, see McCarthy 1993 for a review).

The main difficulty in deciding which is the mechanism responsible for the ultraviolet excess seems to be the low signal-to-noise

⋆Visiting Astronomer at the Cerro Tololo Interamerican Observatory, operated by the Association of Universities for Research in Astronomy, Inc., under contract with the National Science Foundation.

© 1997 RAS

© Royal Astronomical Society • Provided by the NASA Astrophysics Data System

Downloaded from http://mnras.oxfordjournals.org/ at FundaÃ§Ã£o CoordenaÃ§Ã£o de AperfeiÃ§oamento de Pessoal de NÃ-vel Superior on February 27, 2014

1997MNRAS.290..231S

ratio of the observed spectra of these distant radio galaxies. In a recent work Tadhunter, Dickson & Shaw (1996) have obtained good signal-to-noise ratio spectropolarimetry of the relatively nearby radio galaxy 3C 321 ($z \approx 0.1$) and have shown that, besides a red bulge, both a scattered AGN component and a young stellar one are necessary to fit the continuum of this galaxy.

In order to shed some more light on the origin of the continuum in radio galaxies, we investigate in this work, via long-slit spectroscopy, the ultraviolet/optical continuum of the closest powerful radio galaxy: NGC 5128 (Centaurus A), located at only 4 Mpc from the Milky Way (Harris et al. 1992 and references therein, adopted hereafter). General properties are described, for example, in Burns, Feigelson & Schreier (1983 and references therein). In particular, it presents a radio jet which emerges nearly along the major axis of its elliptical stellar component and perpendicular to its prominent dust lane, where several H II regions can be found. There is also X-ray emission from the jet, indicating a common synchrotron radiation origin for the jet emission. The compact core is also a source of γ-ray emission. The outer lobes reach at least 3° (210 kpc) from the nucleus.

Several works have explored optical emission-line spectra of NGC 5128: Phillips (1981) found two types of emission in the nuclear region: one from discrete and diffuse low-ionization H II regions photoionized by O and B stars confined to the dust lane, and the other, more typical of shock-ionized nebulae, found at the nucleus and at the edge of the dust lane in the south-west half of the main elliptical body of the galaxy. Optical emission along the inner jet ($r < 70$ arcsec) has been studied by Brodie, Königl & Bowyer (1983), who found that these regions have emission-line spectra characteristic of shock-heating or photoionization by a power-law continuum. Spectra of the outer optical filaments ($r \approx 8$–15 arcmin) also along the radio jet have been obtained by Morganti et al. (1991), who concluded that these filaments are predominantly photoionized by the radiation field of an AGN continuum, hidden from our direct view.

More recently Schreier et al. (1996), using R and I *Hubble Space Telescope* imaging and polarimetry, obtained $A_V \approx 0.5 - 3.0$ mag throughout the dust lane with peaks of $A_V \approx 7.0$; they also found that the degree of polarization is proportional to extinction.

In this work we explore the nuclear and extra-nuclear spectral properties along the east–west direction, which lies at approximately 40° from the radio axis. We dedicate special attention to the continuum distribution, in particular to the stellar population contribution, since little information is available about this important point for NGC 5128. The paper is structured as follows. In Section 2, we present the observations and reductions, as well as details on the spatial extractions. In Section 3 the spatial properties of the reddening and stellar populations are discussed; in particular, for the nucleus we include the *IUE* spectrum in the analysis. The emission-line spectra are analysed in Section 4, and the conclusions are presented in Section 5.

2 OBSERVATIONS

Observations in the near-ultraviolet and visible ranges were gathered with the 4-m telescope of the Cerro Tololo Inter-American Observatory (CTIO), on the night of 1992 May 30 using the Reticon CCD. They cover the wavelength interval λλ3440–7600 Å with 10-Å spectral resolution. The slit was 10 arcsec wide in order to match the aperture of ultraviolet observations (from *IUE*), since we intended to provide a spectral energy distribution of the nucleus over a wide range of frequencies as in McQuade, Calzetti & Kinney (1995) and Storchi-Bergmann, Kinney & Challis (1995a). The slit was oriented in the east–west direction, and the exposure time was 300 s.

Complementary long-slit near-infrared spectra in the ranges λλ6400–8300 Å and λλ8200–10 000 Å with 5.5-Å spectral resolution were obtained, respectively, on the nights of 1992 May 20 and 22 using the Cassegrain Spectrograph and CCD detector GEC#10 at the 1.5-m telescope of CTIO. Exposure times of 300 s were used in both wavelength ranges. The observations were obtained using the same slit width as that in the 4-m telescope.

The reductions were made using the IRAF software following standard procedures, and the spectra were flux-calibrated using stars from Stone & Baldwin (1983). Owing to non-photometric conditions for the 4-m observations, the corresponding spectra were scaled to the absolute flux level of the near-infrared spectra.

2.1 Spatial extractions

Kunkel & Bradt (1971) identified in the near-infrared (λ≈8000 Å) the nucleus of Cen A with a hotspot which corresponds to a faint feature in the blue. Later, K-band imaging has shown that the nucleus is located 4–6 arcsec south-west of the above location (Giles 1986; Turner, Forrest & Pipher 1992; see also Schreier et al. 1996). We centred the slit on the nucleus as seen in the red-sensitive TV monitor. Since our slit is wide (10 arcsec), we have essentially included the whole nuclear region in our observations.

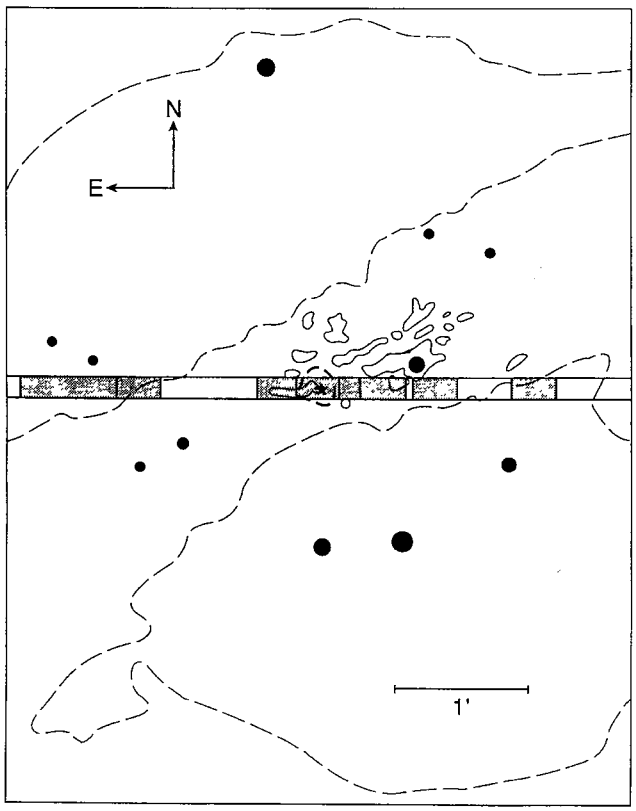

Figure 1. Sketch of the central regions of NGC 5128 with the slit superimposed. Hatched boxes correspond to the positions of the spectral extractions. The dashed contour is the third lowest isophote in Sersic (1967). Blobs in the blue photograph of Kunkel & Bradt (1971) are represented by continuous lines, and the nucleus by a heavy dashed line. Some field stars are also indicated as filled circles.

© Royal Astronomical Society • Provided by the NASA Astrophysics Data System

Downloaded from http://mnras.oxfordjournals.org/ at FundaÃ§Ã£o CoordenaÃ§Ã£o de AperfeiÃ§oamento de Pessoal de NÃ-vel Superior on February 27, 2014

1997MNRAS.290..231S

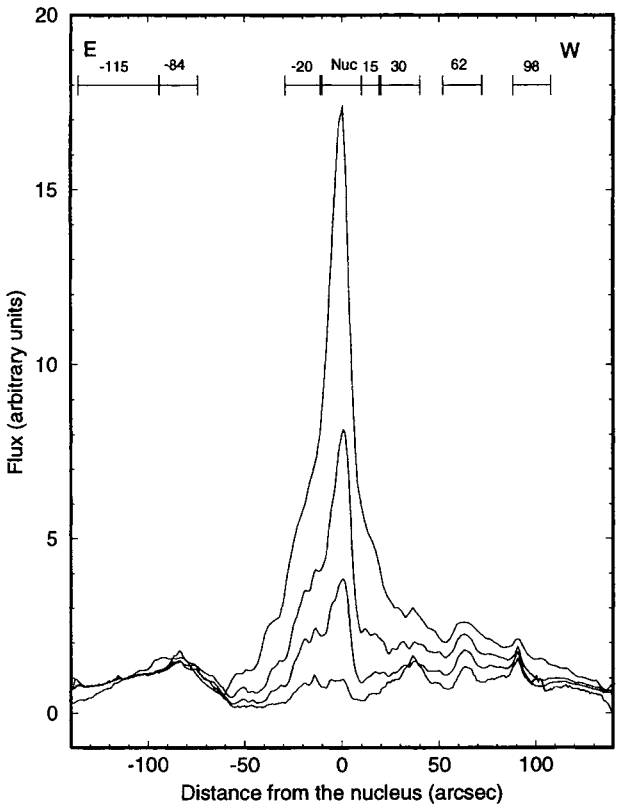

Figure 2. Light profiles along the slit, from bottom to top: λλ3900, 5700, 7300 and 8600 Å. Profiles normalized at ≈110 arcsec E. Positions of the extractions are indicated.

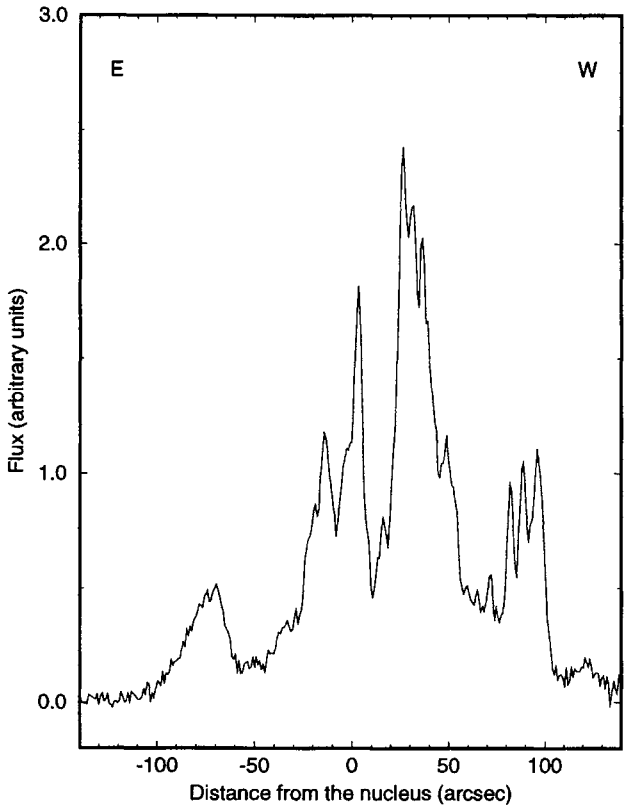

Figure 3. Light profile along the slit at Hα . East is to the left, and west is to the right.

In Fig. 1 we show a schematic representation of the galaxy and the slit. The dashed line corresponds to the third lowest isophotal level of the contour map of NGC 5128 as shown in the Cordoba Atlas of Galaxies (Sersic 1967). On the dust lane, we have represented the brightest features present in the blue photograph shown by Kunkel & Bradt (1971). Also shown as a heavy dashed contour is the location of the hotspot identified by Kunkel & Bradt as the nucleus of the galaxy. The hatched rectangles correspond to the loci of the extracted spectra: one at the nucleus and the others at 14, 30, 62 and 98 arcsec west (W), 15, 52, 84 and 114 arcsec east (E). These locations were selected because they sample the different spectral characteristics of the region covered by the slit. The positions at 14 arcsec W, 15 arcsec E, 30 arcsec W, 52 arcsec E and 62 arcsec W are in the dust lane, whereas positions at 84 arcsec E and 98 arcsec W are on its borders, and finally, position 114 arcsec E samples the stellar population outside the dust lane. The near-infrared (1.5-m) spectra were corrected for atmospheric absorptions using hot comparison stars, following the procedures outlined in Bica & Alloin (1987). The spectra were corrected for foreground (Milky Way) reddening using a Galactic extinction law (Seaton 1979), and adopting $E(B-V)_{\rm f} = 0.043$ which is a value compatible with NGC 5128 globular clusters outside the dust lane (Jablonka et al. 1996). Subsequently they were rebinned to the rest frame with a radial velocity $V_R = 526\,{\rm km\,s^{-1}}$ (Sandage & Tammann 1981).

In Fig. 2 we show light profiles along the slit in four continuum wavelengths: λλ3900, 5700, 7300 and 8600 Å, within spectral windows 50 Å wide. The profiles have been arbitrarily normalized at ≈110 arcsec E of the nucleus. It can be seen that the nucleus is prominent relative to its surroundings at λ8600 Å, whereas it becomes fainter for bluer wavelengths, so that at λ3900 Å it is hardly detectable owing to dust absorption.

In Fig. 3 we show the light profile along the slit at Hα. Comparing this with the continuum profiles in Fig. 2, it can be seen that the strongest emission in Fig. 3 does not correspond to the nucleus, but to a locus at about 30 arcsec W, corresponding to an H II region complex, as discussed in the following sections. Other important Hα emission regions occur at ≈95 arcsec W and ≈85 arcsec E.

In Fig. 4 we show the spectra for the different spatial extractions. Notice how the nucleus and locations in the dust lane are strongly reddened, whereas those at the dust lane borders (84 arcsec E and 98 arcsec W) and beyond (114 arcsec E) are not. As a first attempt to interpret the spectra, we have assumed that the stellar population in the whole central region could be represented by the spectrum corresponding to the extraction at 114 arcsec E, which lies outside the dust lane. The latter spectrum was used as a population template and the other were dereddened with a Galactic extinction law (Seaton 1979) so that the red part of the spectra matched that of the template. We used dust lane colour excess values, $E(B-V)_{\rm dl}$, that give the best match to the template in the near-infrared, since unreddened nuclear stellar populations of different types are basically flat in this spectral region (Bica 1988). These dereddened spectra are shown in Fig. 5. Notice that in most locations along the dust lane, there is a flux excess in the blue as compared to the 114 arcsec E spectrum, indicating that we are not dealing with a simple bulge population reddened by the dust lane, but showing the presence of a young stellar component and/or scattered light associated to the active nucleus (see discussion below). We again stress that the reddening corrections for the spectra in Fig. 5 are

© Royal Astronomical Society • Provided by the NASA Astrophysics Data System

Downloaded from http://mnras.oxfordjournals.org/ at FundaÃ§Ã£o CoordenaÃ§Ã£o de AperfeiÃ§oamento de Pessoal de NÃ-vel Superior on February 27, 2014

1997MNRAS.290..231S

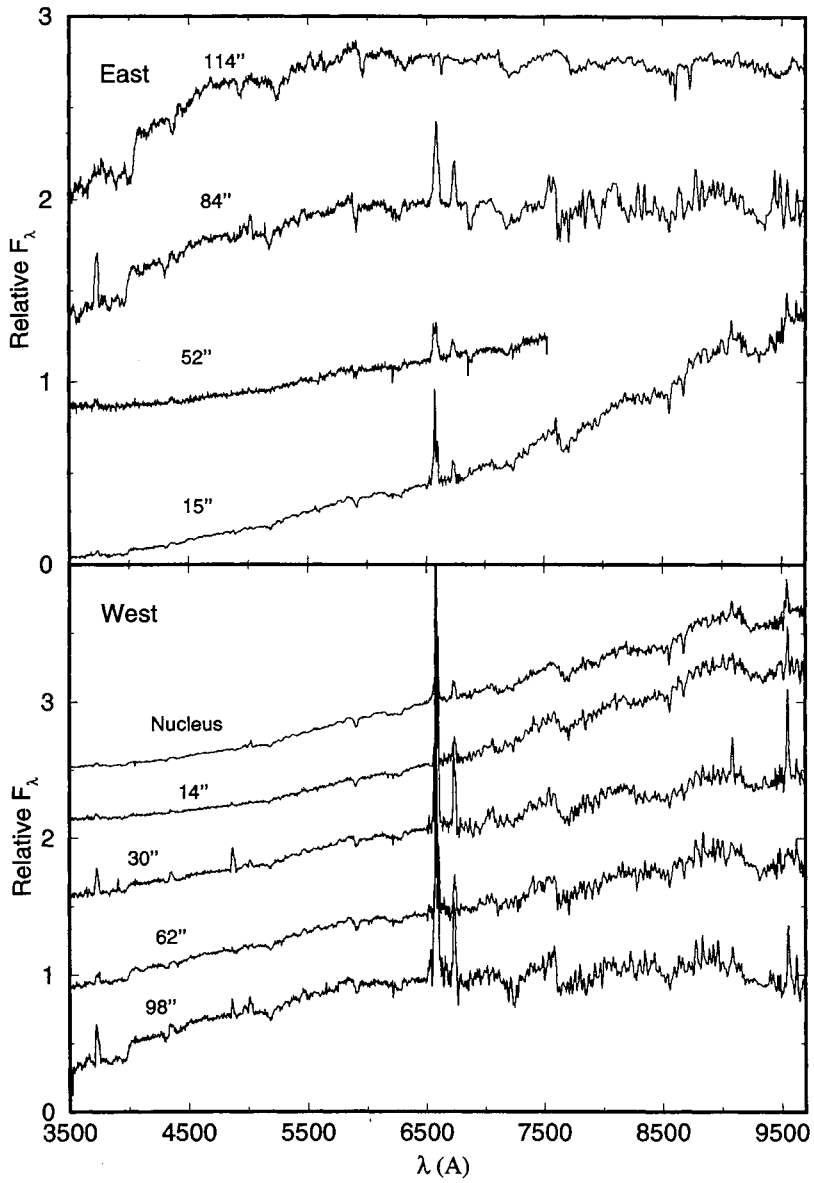

Figure 4. Spectral extractions along the slit. Labels indicate the distance in arcsec from the nucleus. Top panel: locations east of the nucleus; bottom panel: nucleus and locations to the west. Fluxes are in F_λ units normalized at λ8540 Å. Constants have been added to the spectra for clarity, except for the bottom ones.

preliminary, and that a better description is provided by composite models, including differentially reddened components (Section 3).

3 SPATIAL DEPENDENCE OF REDDENING, STELLAR POPULATION AND SCATTERED LIGHT

We have measured equivalent widths (*W*) of the strongest absorption atomic lines and molecular bands using the windows and continuum points from Bica & Alloin (1986a,b, 1987). The results are shown in Table 1. For the 4-m spectra, the signal-to-noise ratio is very high, and the errors in *W*s are typically 5 per cent; for the 1.5-m spectra outside the nucleus, they increase to ≈10 per cent, or more in a few cases which are marked with a colon in Table 1.

We show in Fig. 6 the *W*s as a function of distance from the nucleus. Diagnostics of the stellar populations can be made by comparing the measured values with those of template spectra for a wide range of populations found in nuclear regions of galaxies (Bica 1988).

It can be seen that the Ca II K line has a value of ≈13 Å in the nucleus, decreases to ≈6 Å for intermediate distances, and increases again outwards to ≈15 Å outside the dust lane. A similar behaviour occurs for the G band and Mg I+MgH. Such weakening of metallic lines could be interpreted as a result of a low metallicity, the presence of low-age components, and/or dilution by a blue AGN continuum. On the other hand, in the near-infrared, the calcium triplet is strong and approximately constant throughout the slit, indicating high metallicities like those found in the nuclei of elliptical and spiral galaxies (Bica 1988). TiO values in the red (Table 1) are consistent with metallic populations, especially for the central regions. Consequently, Ca II K, G band and Mg I *W*s indicate the presence of dilution by a blue–green continuum, except for the outermost extraction (114 arcsec E, outside the dust lane), which

© Royal Astronomical Society • Provided by the NASA Astrophysics Data System

Downloaded from http://mnras.oxfordjournals.org/ at FundaÃ§Ã£o CoordenaÃ§Ã£o de AperfeiÃ§oamento de Pessoal de NÃ-vel Superior on February 27, 2014

1997MNRAS.290..231S

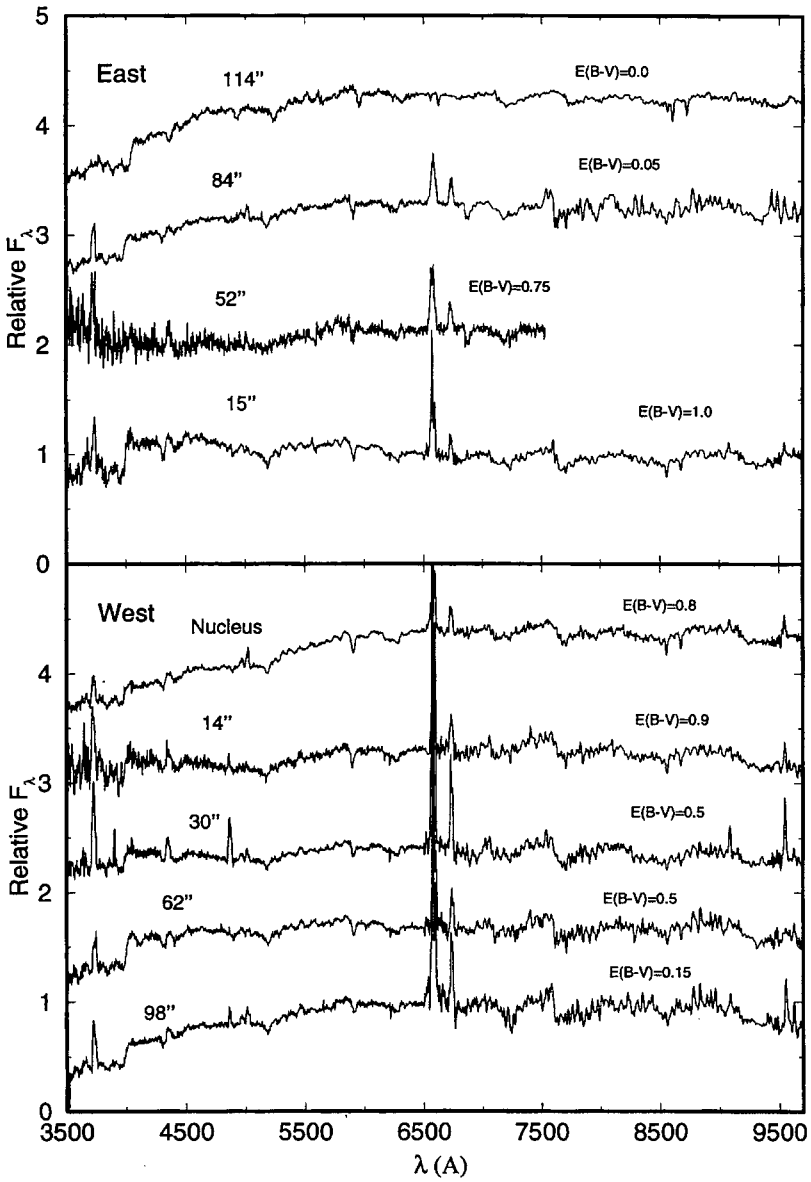

Figure 5. Same as Fig. 4 but reddening corrected with the Galactic extinction law and excess $E(B-V)_{dl}$ to match the near-infrared range of the spectrum 114.″5 E (outside the dust lane). Notice how these simple guesses produce important flux excesses in the blue for the extractions along the dust lane, suggesting the presence of a young stellar population component.

shows values typical of a bulge population. This diluting continuum can be directly observed in the tentatively dereddened spectra (Fig. 5) as blue flux excesses, especially for locations in the dust lane for which $r \leq 52$ arcsec. Blue–green *W*s for the nucleus are not consistent with pure bulges of giant ellipticals, being diluted by ≈25 per cent at λ3950 Å.

In principle, both very young (H II regions) and non-thermal continua have similar spectral distributions in the optical region, and can dilute metallic lines. Star clusters as young as 5 Myr already develop Ca II triplet (Bica, Alloin & Santos 1990), and are able to dilute in the blue but conserving the *W*s of calcium in the near-infrared. Dilution in the blue, but not in the near-infrared, can thus be obtained by substantial occurrence of ageing blue stellar populations older than 5 Myr. Since compact H II regions have been observed throughout the dust lane (Graham 1979), it is probable that evolving complexes also occur. On the other hand, it has been shown that radio galaxies can present a very steep power-law spectrum in polarized light probably originating from scattered nuclear light (Tadhunter et al. 1996) which dilutes absorption features preferentially in the blue. Direct light from the active nucleus is not expected to be observed owing to the enormous extinction (Feigelson et al. 1981; Schreier et al. 1996). A possible discriminant, although requiring a high signal-to-noise ratio and spectral resolution, would be the presence of high-order Balmer features that do not suffer substantial emission contamination and trace recent star formation events (although older than H II regions).

It is worth noting (Fig. 6) that the nuclear and adjacent spectra have values of *W*(Ca II triplet) comparable to those of the bulge outside the dust lane (114 arcsec E). Besides the dilution effects discussed above, this could be a result of an absence of metallicity gradient in this galaxy.

© Royal Astronomical Society • Provided by the NASA Astrophysics Data System

Downloaded from http://mnras.oxfordjournals.org/ at FundaÃ§Ã£o CoordenaÃ§Ã£o de AperfeiÃ§oamento de Pessoal de NÃ-vel Superior on February 27, 2014

1997MNRAS.290..231S

Table 1. Equivalent widths.

Main Absorber	Window (Å)	Nucleus	14″ West	30″ West	62″ West	98″ West	−15″ East	−52″ East	−84″ East	−114″ East
Ca II K	3908–3952	12.9	10.5	5.4	9.6	10.6	11.7	4.8	9.9	15.0
Hδ	4082–4124	5.4	3.7	2.0	4.3	1.8	4.2	5.5:	3.8	4.2
CN	4150–4214	7.9	4.8	2.2	3.1	3.5	5.6	6.8:	3.4	4.3
G band	4284–4318	6.3	4.1	2.8	4.3	4.1	5.3	4.3:	4.6	5.8
Hγ	4318–4364	3.2	0.0	−1.8	3.3	0.2	4.0	0.6:	3.4	4.7
Hβ	4846–4884	2.1	−0.2	−8.1	1.8	−1.9	1.7	0.3	1.5	4.1
MgH	5130–5156	2.9	2.8	1.5	1.9	2.2	2.3	1.7	1.3	2.4
Mg I+MgH	5156–5196	6.9	5.2	4.0	4.9	5.3	5.9	3.1	4.9	6.2
MgH	5196–5244	4.6	3.0	2.2	3.4	2.9	3.9	2.0	3.0	4.9
Na I	5880–5914	5.4	4.8	3.3	4.0	3.3	4.2	4.7	4.2	4.2
TiO	6156–6386	18.1	23.5	13.7	14.8	11.7	15.4	17.2	11.4	12.9
Hα	6540–6586	−13.6	−24.7	−76.8	−29.3	−47.4	−20.5	−19.0	−11.9	2.0
TiO	7050–7464	31.3	30.0	36.1	34.0	48.2	29.5	28.7	36.3	27.2
Ca II	8476–8520	5.2	4.6	6.5	5.4	6.9:	4.7	–	5.7:	5.6
Ca II	8520–8564	6.7	6.8	6.9	6.7	8.4:	6.7	–	7.5:	7.0
Ca II	8640–8700	5.5	4.7	6.3	5.7	5.6:	5.4	–	5.6:	5.6

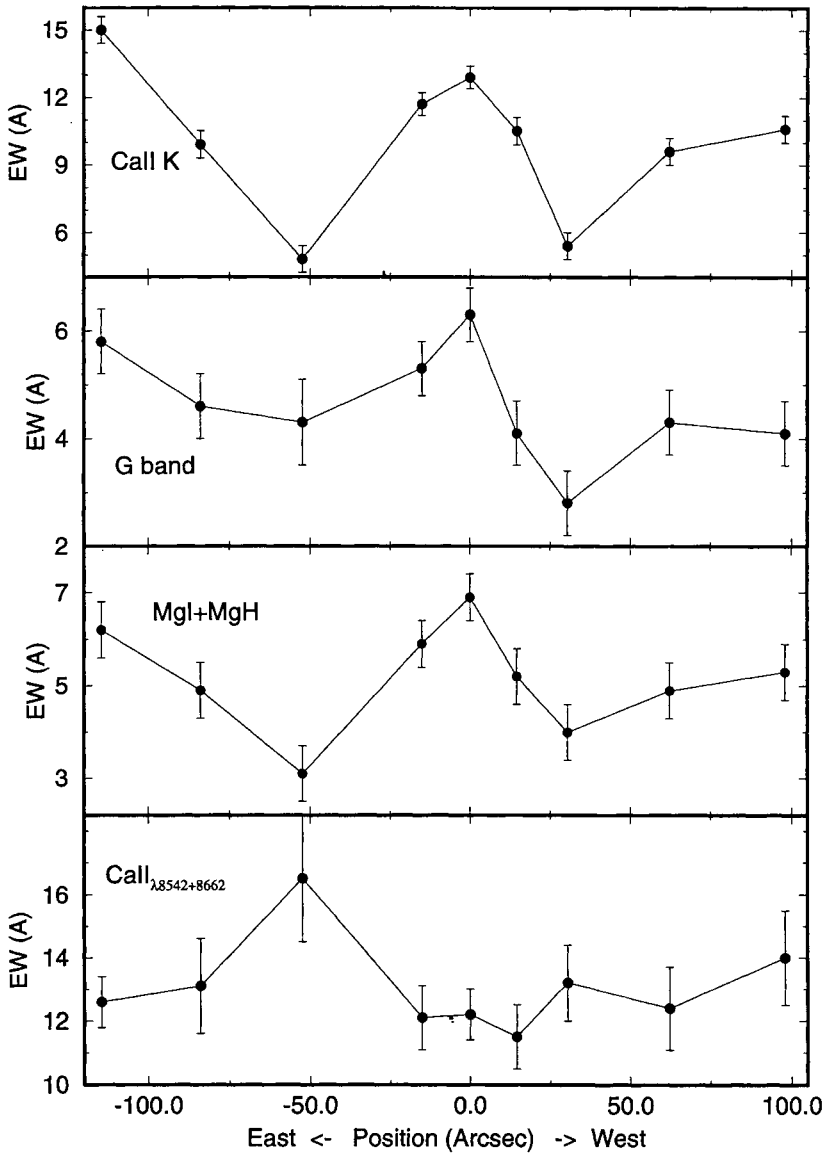

Figure 6. Equivalent widths of prominent spectral absorption features as a function of position.

© Royal Astronomical Society • Provided by the NASA Astrophysics Data System

Downloaded from http://mnras.oxfordjournals.org/ at FundaÃ§Ã£o CoordenaÃ§Ã£o de AperfeiÃ§oamento de Pessoal de NÃ-vel Superior on February 27, 2014

1997MNRAS.290..231S

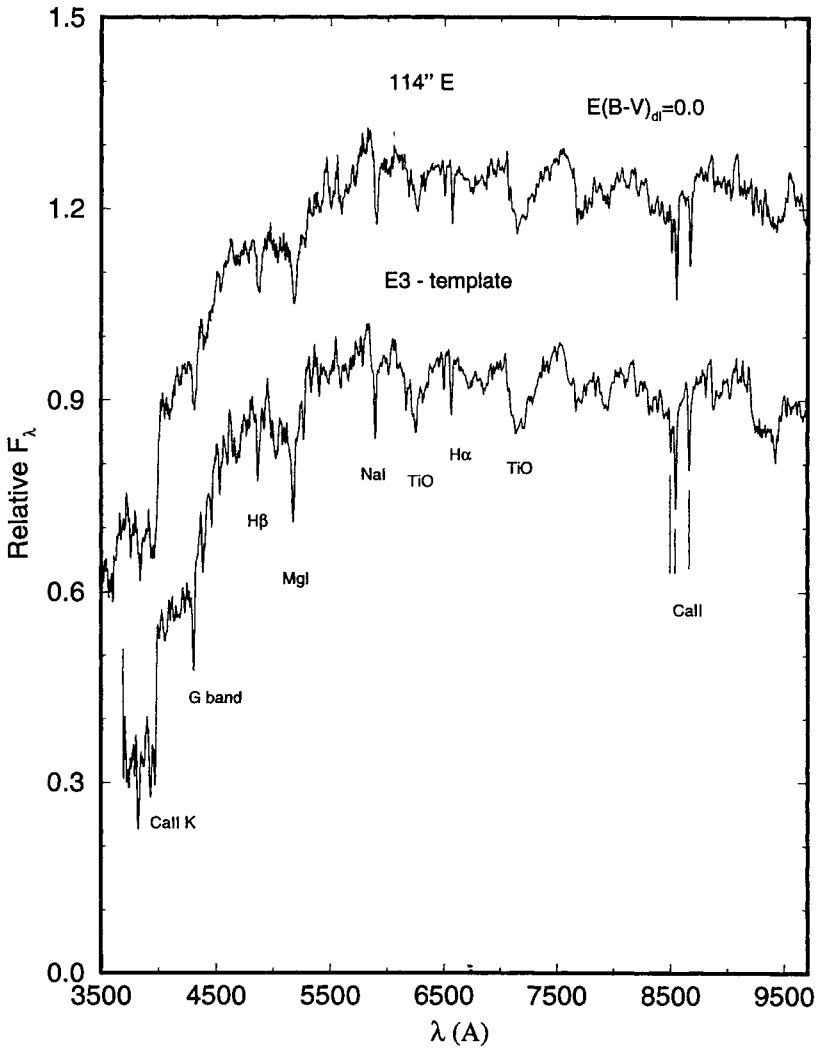

Figure 7. Extraction 114 arcsec E (top) compared to the E 3 template (bottom). Main absorption lines are identified. Flux in F_λ units normalized at λ5870 Å. A constant has been added to the upper spectrum for clarity.

3.1 Syntheses of individual spectra

In this section we perform a simple synthesis of each extracted spectrum. As can be seen in the tentatively dereddened spectra in Fig. 5, a typical bulge stellar population component must be present in all cases. The first step was trying a match of the *W*s of the observed spectrum with those of one of the usual galaxy population templates, and subsequently finding the reddening which best reproduces the continuum distribution. For the cases which could not be described by this simple approach, we used composite models considering the possible contributions of: (i) a bulge stellar population typical of elliptical galaxies; (ii) a blue stellar population associated to the dust lane disc; and (iii) a power-law component to represent scattered blue light from the nucleus. In all cases we allowed for different amounts of reddening affecting each component.

Although in principle the three components may occur simultaneously, we verified that, within our signal-to-noise ratio, at most two components were necessary to give a satisfactory fit to the data.

In the case that the diluting continuum is scattered nuclear light, we have represented it by a power law $F_\lambda \propto \lambda^{-\alpha}$, with a slope α obtained with the following expression:

$$-\alpha = \frac{\log(F_{P2}/F_{P1}) + \log[(W_{P2}/W_2 - 1)/(W_{P1}/W_1 - 1)]}{\log(\lambda_2/\lambda_1)},$$

where F_{P2}, F_{P1} and W_{P2} and W_{P1} are, respectively, the continuum levels and equivalent widths of two absorption features at λ_2 and λ_1 of the adopted bulge *stellar population* template, and W_2 and W_1 are the corresponding observed equivalent widths. We chose as features 1 and 2 respectively, K Ca II and Mg I+Mg H in order to have both the longest wavelength baseline and good signal-to-noise ratio.

The results of the individual syntheses are described below.

3.1.1 Extraction 114 arcsec E

For this locus outside the dust lane, the equivalent widths and continuum are best described by a typical bulge population of elliptical galaxies with solar metallicity (E 3 template in Bica 1988), with no need to include a blue diluting continuum. We compare this spectrum with the E 3 template in Fig. 7. No additional reddening other than the small foreground value (Section 2.1) is necessary.

© Royal Astronomical Society • Provided by the NASA Astrophysics Data System

Downloaded from http://mnras.oxfordjournals.org/ at FundaÃ§Ã£o CoordenaÃ§Ã£o de AperfeiÃ§oamento de Pessoal de NÃ-vel Superior on February 27, 2014

1997MNRAS.290..231S

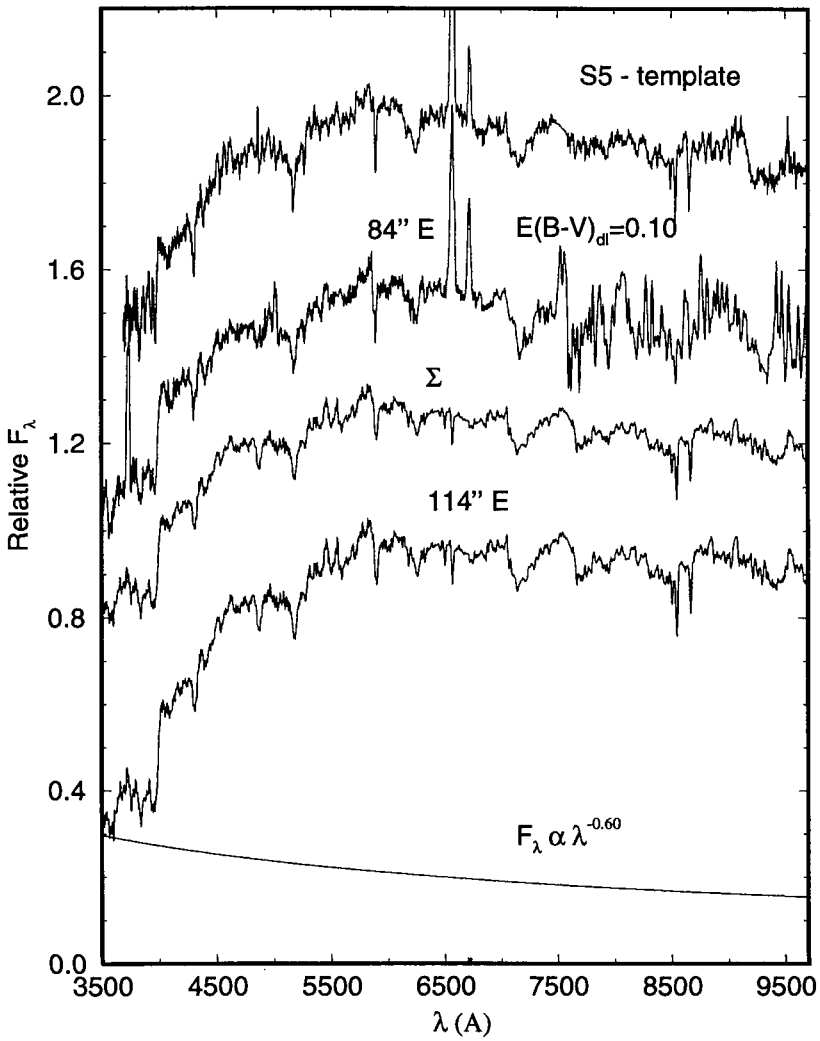

Figure 8. Synthesis of extraction 84 arcsec E. From bottom to top: the power-law component, the adopted bulge population, and their sum compared with the observed 84 arcsec E spectrum corrected by $E(B-V)_{dl} = 0.10$, and the S 5 population template. The spectra have been shifted by arbitrary constants, except for two bottom ones which are shown in the actual proportions used for the synthesis.

3.1.2 Extractions 84 arcsec E and 98 arcsec W

The best stellar population match for these extractions is the template S 5 with reddenings arising in the dust lane $E(B-V)_{dl} = 0.10$ and 0.20, respectively. We illustrate the case of extraction 84 arcsec E in Fig. 8. However, better matches for these extractions are obtained for the bulge population outside the dust lane (114 arcsec E) combined to power laws of slope $\alpha = 0.6$ and 1.5, respectively, with excesses $E(B-V)_{dl} = 0.10$ and 0.30. The power-law contributions amount to 34 and 30 per cent, respectively, at the K Ca II continuum. Both the S 5 template and the synthesis with a power law reproduce the observed dilution of metallic line *W*s, but the latter approach describes best the 4000-Å break (Fig. 8). Interestingly these two extractions lie at the borders of the dust lane (Figs 1 and 2) where the extinction is low. The dust in these loci probably act as mirrors that scatter the nuclear light producing the observed blue continuum.

3.1.3 Extraction 62 arcsec W

The best stellar population match for this extraction is the template S 6 with $E(B-V)_{dl}$=0.50. The synthesis of bulge plus a power law gives $\alpha = 1.0$, with 36 per cent contribution of the power law at the K Ca II continuum. However, the pure stellar population template S 6 describes better the 4000-Å break and continuum in the range 4000–4500 Å.

The galaxy template S 6 is made up of 24 per cent (flux at λ5870 Å) of stellar populations younger than 500 Myr, 6 per cent of intermediate age components (1–5 Gyr), and 70 per cent of old ones (≥10 Gyr), attaining solar metallicity (Bica 1988). This indicates the presence of recent star formation in the dusty disc (in agreement with Graham's 1979 detection of H II regions); star formation events in the disc may have occurred for ages as high as 1 Gyr. We conclude that extinction at this more central locus blocks considerably more light from the bulge (and some eventual scattered nuclear light), making young components from the foreground regions of the disc responsible for the dilution effects.

3.1.4 Extractions 30 arcsec W and 52 arcsec E

An inspection of Fig. 5 where we tentatively dereddened these spectra, shows a broad dip between λλ4750 and 5200 Å, which is further enhanced by the MgH absorption around the $Mg\,I_{\lambda 5175}$

© Royal Astronomical Society • Provided by the NASA Astrophysics Data System

Downloaded from http://mnras.oxfordjournals.org/ at FundaÃ§Ã£o CoordenaÃ§Ã£o de AperfeiÃ§oamento de Pessoal de NÃ-vel Superior on February 27, 2014

1997MNRAS.290..231S

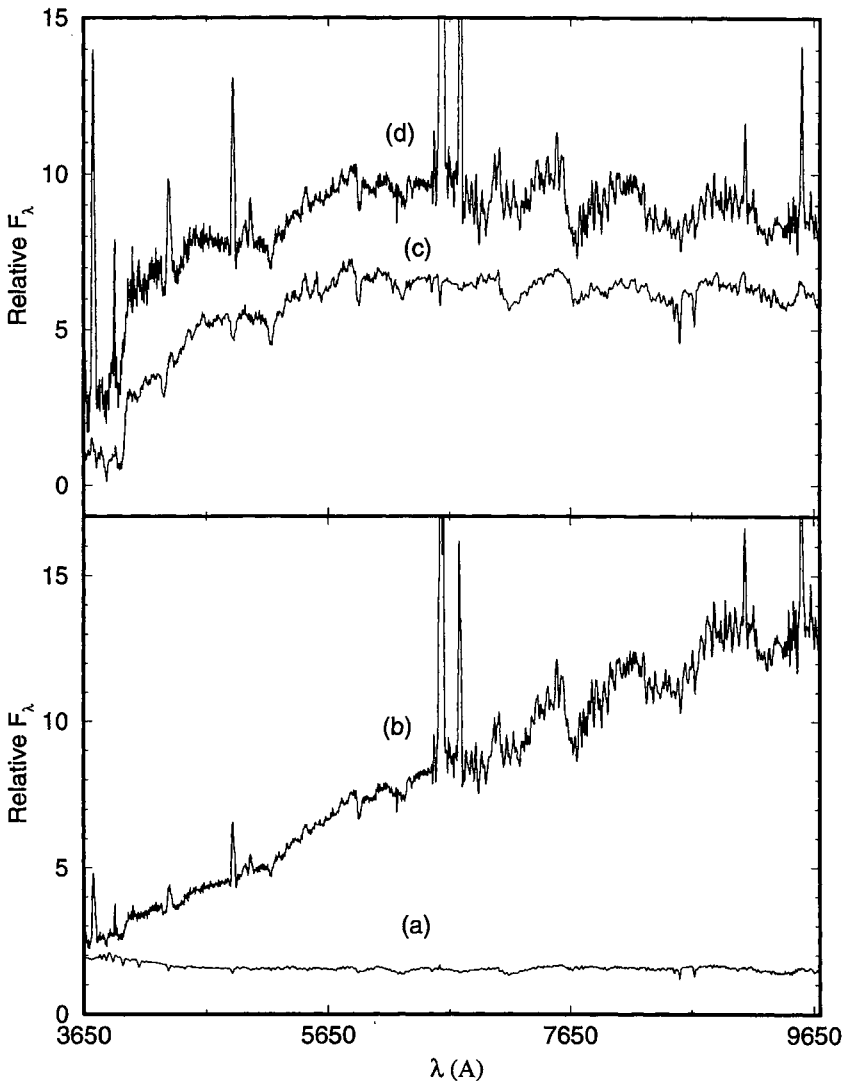

Figure 9. Synthesis of extraction 30 arcsec W. (a) Model: 'disc' population reddened with $E(B-V) = 0.20$; (b) observed spectrum from extraction 30 arcsec W; (c) 114 arcsec E (bulge population); and (d) extraction 30 arcsec W after subtraction of the 'disc' population, and dereddened with $E(B-V)_{dl} = 0.60$. Flux in F_λ units normalized at λ5870 Å. A constant has been added to spectrum (d) for clarity.

feature. None of the galaxy templates matches the broad dip. It is not present either in any star cluster spectrum (Bica 1986a). Such a dip can be reproduced by the combination of a steep red spectrum and a steep blue one. This seems to be the case of the central regions of Cen A where a prominent bulge population is further reddened with respect to a foreground disc population mixed with dust. In order to test this possibility, we have simulated a disc spectrum composed of 20 per cent (flux fraction at λ5870 Å) of an H II region continuum and 80 per cent of the Y 1 star cluster template of Bica (1988) with an age of ≈10 Myr. Such a disc is able to reproduce the observed dilution of blue absorption features and at the same time preserve the strength of the molecular bands in the near-IR. The Y 1 template corresponds to the phase with red supergiants which contain molecular bands as strong as those of the bulge stellar population. Subsequently, we combined this 'disc' with a bulge stellar population represented by the spectrum 114 arcsec E. We tried to reproduce the overall continuum distribution using different proportions and reddening amounts for each component. As a constraint we used the observed dilution of the blue–green metallic lines (Table 1).

The best match obtained for extraction 30 arcsec W is shown in Fig. 9. As it lies in the foreground, the 'disc' spectrum was assumed to be less reddened, and the best result was obtained with $E(B-V) = 0.20$. The resulting disc spectrum was scaled to 60 per cent of the observed K Ca II continuum flux (30 per cent at Mg I+MgH) and subtracted. This factor corresponds to the dilution of the bulge spectrum by the adopted disc, in order to reproduce the observed *W*s in the region. The subtracted spectrum was dereddened with $E(B-V)_{dl} = 0.60$ which can be compared to the bulge population spectrum in Fig. 9.

Considering the signal-to-noise ratio of our data, the spectral distribution of extraction 52 arcsec E matches that of the 30 arcsec W, but with an additional reddening correction of $\Delta E(B-V) = 0.15$ (Fig. 5). Consequently the same model can be assumed.

On the other hand, the syntheses of a bulge plus a power law give $\alpha = 2.5$ (contributing with 64 per cent of the continuum flux at K Ca II continuum) and $\alpha = 1.0$ (68 per cent at K Ca II), respectively for the locations 30 arcsec W and 52 arcsec E. For the former extraction there remains a continuum excess in the

© Royal Astronomical Society • Provided by the NASA Astrophysics Data System

Downloaded from http://mnras.oxfordjournals.org/ at FundaÃ§Ã£o CoordenaÃ§Ã£o de AperfeiÃ§oamento de Pessoal de NÃ-vel Superior on February 27, 2014

1997MNRAS.290..231S

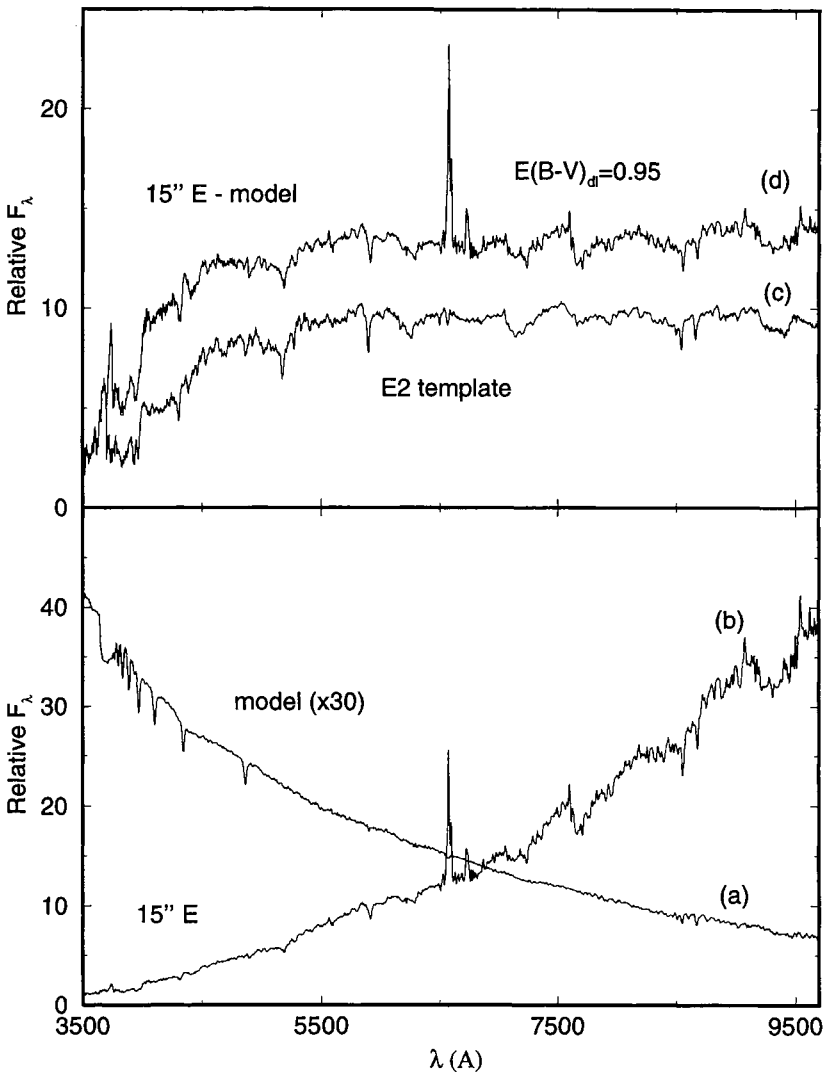

Figure 10. Synthesis of extraction 15 arcsec E. (a) Model: 'disc' population reddened with $E(B-V) = 0.10$ and multiplied by a factor 30 for visualization purposes; (b) observed spectrum from extraction 15 arcsec E; (c) E 2 (bulge population) template; and (d) extraction 15 arcsec E after subtraction of the 'disc' population, and dereddened with $E(B-V)_{dl} = 0.95$. Flux in F_λ units normalized at λ5870 Å. A constant has been added to spectrum (d) for clarity.

region 4000–4500 Å that cannot be described by the bulge plus power law model. This kind of excess can only be accounted for by the contribution of a young stellar component, similar to what was found by Tadhunter et al. (1996) for the radio galaxy 3C 321.

3.1.5 Extractions 15 arcsec E and 14 arcsec W

Similarly to extraction 30 arcsec W, these two spectra show the broad dip between λλ4750–5200 Å, and consequently also require a composite model. Since these locations are very close to the nucleus, we have adopted as representative of the bulge population component the E 2 template, which has a higher than solar metallicity (Bica 1988) and matches the nuclear bulge population (see Section 3.2). The E 2 template is suitable for central regions of giant ellipticals (Bica 1988).

We have adopted a disc population with a wider range of ages than that used for the 30 arcsec W extraction. This can be justified because the present line of sight is closer to the centre and should sample a larger number of age components throughout the disc. This disc is composed of 60 per cent of an H II region continuum (flux fraction at λ5870 Å) and 40 per cent of the Y 2 star cluster template of Bica (1988) with an age of ≈50 Myr. The basic difference between the present disc model and the previous one is the lack of red supergiant features which is compensated by the presence of stronger TiO in the metal-rich E 2 template.

The best match obtained for extraction 15 arcsec E is shown in Fig. 10. As it lies in the foreground, the 'disc' spectrum was assumed to be less reddened, and the best match was obtained with $E(B-V) = 0.10$. The resulting disc spectrum was scaled to 50 per cent of the flux in the region of Ca II K relative to that of extraction 15 arcsec E, and subtracted. This factor corresponds to the dilution of an E 2 template by the adopted disc spectrum, in order to reproduce the observed *W*s. The subtracted spectrum was dereddened with $E(B-V)_{dl} = 0.95$, which can be compared to the E 2 (bulge population) template in Fig. 10.

The synthesis of extraction 14 arcsec W is the same as that of 15 arcsec E, with $E(B-V)_{dl} = 1.0$ applied to deredden the disc-subtracted spectrum.

© Royal Astronomical Society • Provided by the NASA Astrophysics Data System

Downloaded from http://mnras.oxfordjournals.org/ at FundaÃ§Ã£o CoordenaÃ§Ã£o de AperfeiÃ§oamento de Pessoal de NÃ-vel Superior on February 27, 2014

1997MNRAS.290..231S

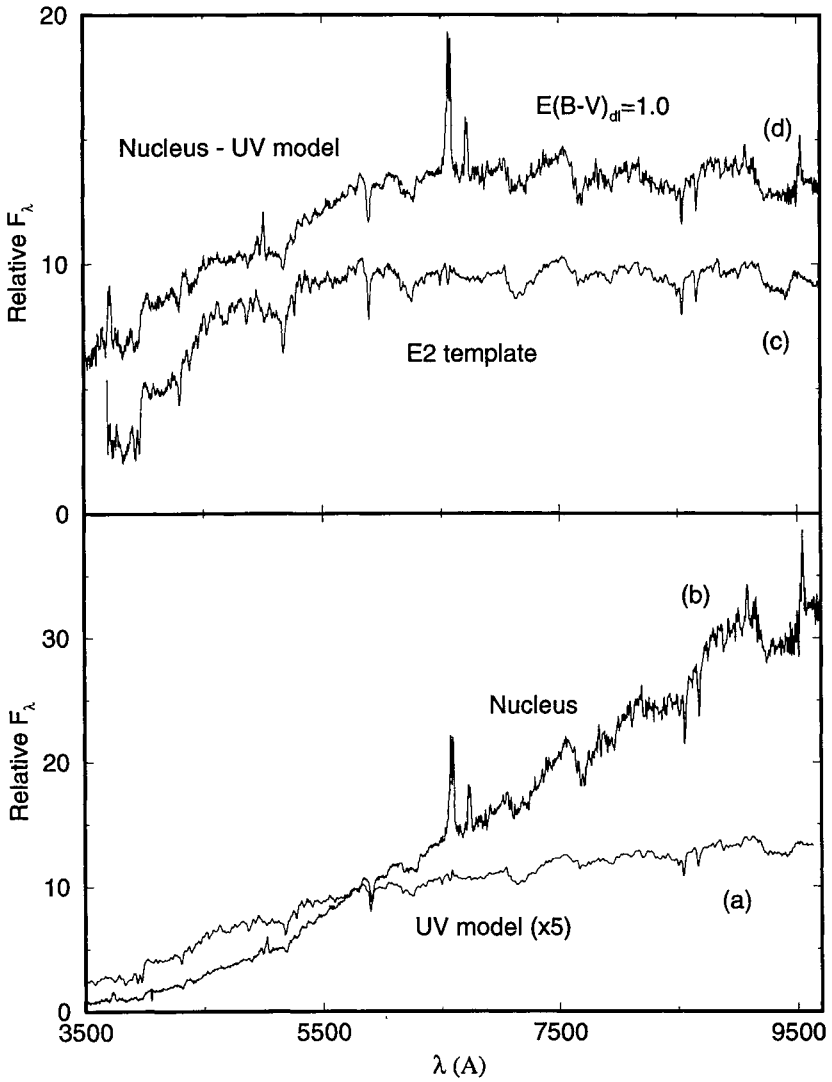

Figure 11. Synthesis of the nuclear spectrum. (a) Disk and foreground bulge parts derived from the ultraviolet (Bonatto et al. 1996); flux scale multiplied by 5 for visualization purposes; (b) observed nuclear spectrum; (c) E 2 (bulge population) template; and (d) nuclear spectrum after subtraction of the disc population + foreground parts of the bulge, and reddening corrected with $E(B-V)_{dl}$=1.0. Flux in F_λ units normalized at λ5870 Å. A constant has been added to spectrum (d) for clarity.

The syntheses of a bulge (E 2) plus a power law give $\alpha = 1.2$ for both locations 15 arcsec E and 14 arcsec W. The corresponding flux fractions at K CaII are 32 and 39 per cent, respectively. Nevertheless, this model cannot account for the continuum excess in the region 4000–4500 Å, similar to what was observed in the 30 arcsec W spectrum.

3.2 The nuclear spectrum

Bonatto et al. (1996) have gathered all available *IUE* spectra of NGC 5128 and constructed an average spectrum of its nuclear region, after discarding a few spectra that were too bright and seemed to correspond to a foreground A star, and another to an H II region. They concluded that the nuclear stellar population in the ultraviolet is best described by a combination of a disc population (similar to that used in the synthesis of extraction 15 arcsec E, Fig. 10), and a red (bulge) one, reddened with an SMC extinction law (Bouchet et al. 1985) and $E(B-V)_{dl} = 0.30$. This mixture would be the result of foreground regions of the bulge which coexist spatially with the disc. The SMC law applies, since there is no evidence of the λ2200 Å bump (Bonatto et al. 1996).

Although observed with equivalent apertures, the absolute flux of the *IUE* spectrum differs by a factor of ≈2 from that of the present optical spectrum at the connecting wavelength (≈3300 Å). Consequently, the *IUE* spectrum was scaled to match the blue end of the present optical data.

We have adopted the ultraviolet synthesis of Bonatto et al. (1996) to construct a corresponding synthetic optical spectrum to represent the disc component. This component was subsequently subtracted from the nuclear spectrum, as shown in Fig. 11 (bottom panel). In the difference spectrum, the W(Ca II K) is ≈25 per cent larger than that in the observed one, and similar to that from an old metal-rich bulge, represented by the E 2 template (Bica 1988). In order to obtain a continuum distribution similar to that of the E 2 template, it was necessary to deredden the difference spectrum by $E(B-V)_{dl} = 1.0$, which can be interpreted as originating in deeper layers of the bulge. The result of this procedure is shown in Fig. 11 (top panel).

© Royal Astronomical Society • Provided by the NASA Astrophysics Data System

Downloaded from http://mnras.oxfordjournals.org/ at FundaÃ§Ã£o CoordenaÃ§Ã£o de AperfeiÃ§oamento de Pessoal de NÃ-vel Superior on February 27, 2014

1997MNRAS.290..231S

Table 2. Relative emission-line fluxes.

Emission Line	Nucleus	14″ West	30″ West	62″ West	98″ West	−15″ East	−52″ East	−84″ East
[O II]$_{\lambda 3727}$	102.1	51.9	58.8	64.6	33.9	74.8	189.0	97.3
Hβ	19.6	22.2	30.0	12.2	12.5	15.9	46.3	16.2
[O III]$_{\lambda 5007}$	59.7	10.0	5.6	5.6	11.9	11.7	41.8	22.8
Hα	100.0	100.0	100.0	100.0	100.0	100.0	100.0	100.0
[N II]$_{\lambda 6583}$	85.0	43.1	38.6	35.3	37.6	44.0	100.0	67.8
[S II]$_{\lambda 6717}$	32.6	18.3	16.2	21.7	34.2	23.4	32.8	56.3
[S II]$_{\lambda 6732}$	32.7	24.4	11.0	13.4	17.0	13.1	28.1	16.9
[S III]$_{\lambda 9069}$	15.5	5.7	4.5	–	7.2	3.5	–	7.7
[S III]$_{\lambda 9532}$	41.5	17.0	10.2	–	22.2	10.5	–	29.4

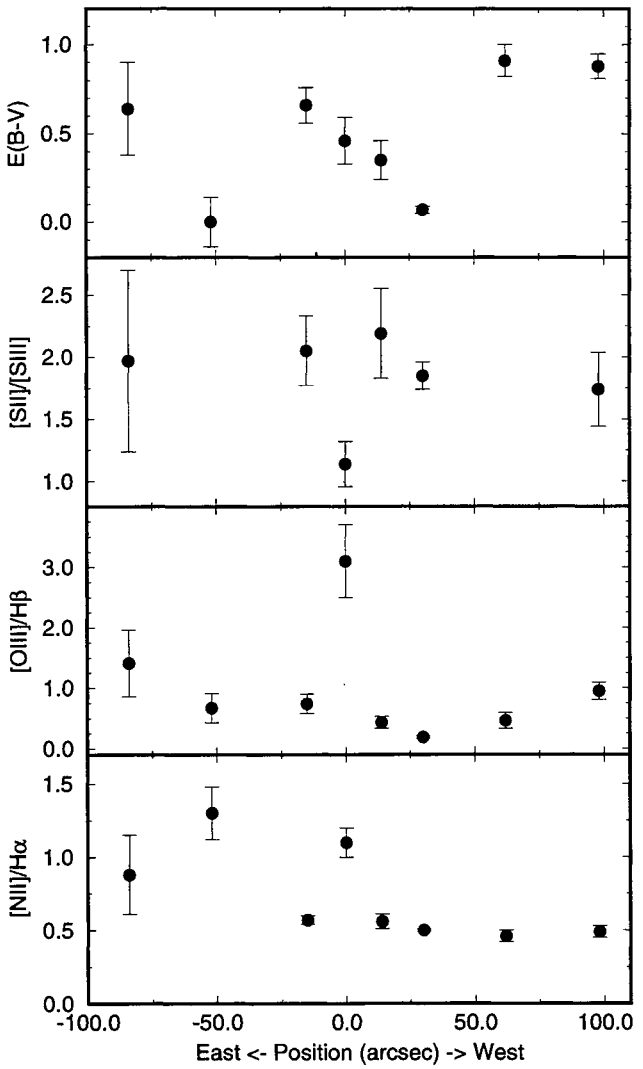

Figure 12. Spatial variation of selected emission-line ratios and internal colour excess derived from Hα/Hβ (top panel).

For the nuclear spectrum, the power law which best reproduces the observed dilutions has slope $\alpha = 0.7$ and contributes with ≈25 per cent of the flux at K Ca II. The combination of this power-law with the E 2 template gives an equivalent fit of the optical features: 4000-Å break, *Ws* and continuum. However, the presence of stellar features in the ultraviolet spectrum (Bonatto et al. 1996) argues in favour of the disc model for the optical.

In summary, the population syntheses of the nucleus and extranuclear extractions show that there is a significant contribution from a red bulge population which dominates the flux for λ≥5500 Å, in all locations. The power-law component dominates the blue continuum at the interface of the dusty disc and the bulge. For the more internal spectra throughout the dusty disc, the blue component is dominated by regions of recent star formation, located at different depths within the dust lane. The latter result is consistent with the evidence that: in all spectra the Ca II triplet is not significantly diluted; stellar absorption features are present in the *IUE* nuclear spectrum (Bonatto et al. 1996); and finally several visible emission-line spectra along the dust lane are characteristic of H II regions (Section 4). Nevertheless, it is worth noting that the young component used in the syntheses discussed above has contribution of H II region continuum, the general shape of which in the optical can also be reproduced by a power law. This means that some fraction of scattered light may also be present in the adopted H II region continuum at these more internal locations.

4 EMISSION LINES

The emission lines in each extracted spectrum were measured after the subtraction of the corresponding synthetic stellar population templates (Section 3), and their values are listed in Table 2. The subtraction of the stellar population is fundamental, in particular for Hβ (Bonatto et al. 1989). Errors in the fluxes have been estimated according to the rms deviation of the adjacent continuum to each line multiplied by the FWHM of the line. They amount to ≈5 per cent for all the lines except for [O II]$_{\lambda 3727}$ for which the error is ≈10 per cent; for extractions 52 arcsec E and 84 arcsec E the errors are twice these values. Fig. 12 illustrates the spatial variation of selected line ratios, as well as the gaseous internal colour excesses, adopting an intrinsic $H\alpha/H\beta = 3.1$ (Osterbrock 1989). Error bars were calculated according to the errors in the fluxes, as estimated above. The highest excitation spectrum corresponds to the nucleus, with line ratios typical of shock-ionized gas (or LINER, Heckman 1980), whereas most extranuclear spectra are consistent with H II region line ratios.

The reddening values derived from the Balmer decrement in Fig. 12 reflect the reddening intrinsic to the gas, after corrections for the foreground (Section 2) and the reddening internal to the dust lane (Section 3). It is interesting to notice that the spectra with the lowest intrinsic reddening present blue continua (Fig. 5) and

© Royal Astronomical Society • Provided by the NASA Astrophysics Data System

Downloaded from http://mnras.oxfordjournals.org/ at FundaÃ§Ã£o CoordenaÃ§Ã£o de AperfeiÃ§oamento de Pessoal de NÃ-vel Superior on February 27, 2014

1997MNRAS.290..231S

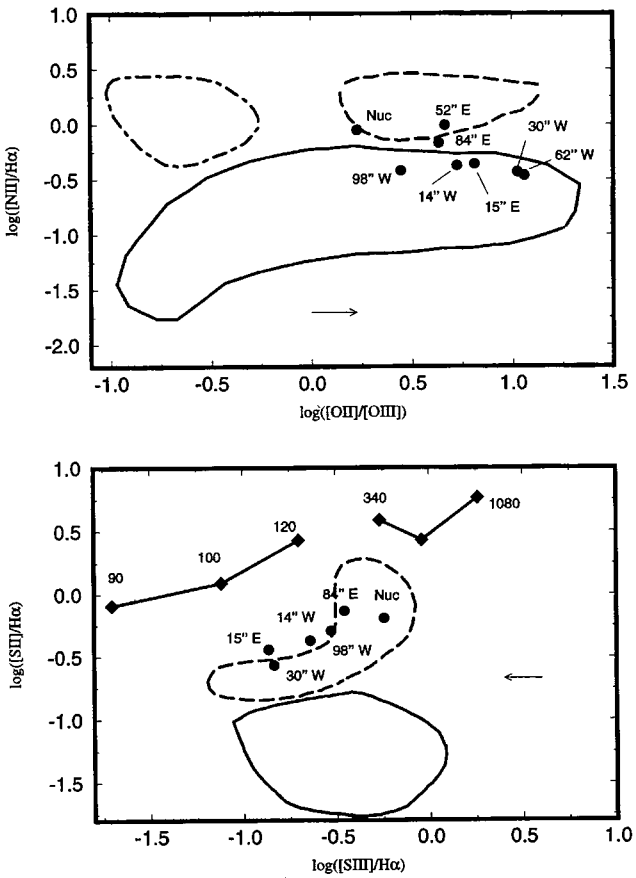

Figure 13. Top panel: diagnostic-diagram log ($[N\,II]_{\lambda6584}/H\alpha$) × log($[O\,II]/[O\,III]_{\lambda5007}$), adapted from Baldwin, Phillips & Terlevich (1981). Bottom panel: diagnostic-diagram log ($[S\,II]_{\lambda\lambda6717,6731}/H\alpha$)×log ($[S\,III]_{\lambda\lambda9069,9532}/H\alpha$), adapted from Diaz et al. (1985). The closed continuous line delineates the area occupied by H II regions; the dashed line, that occupied by LINERs; and the dot-dashed, objects photoionized by power-law spectra. Squares linked by heavy lines represent shock models, and the numbers are the corresponding shock velocities in km s^{-1}. Typical reddening corrections from Hα/Hβ (Table 2) are illustrated by the arrows.

probably originate near the outer border of the dusty disc. The other spectra apparently originate from regions deeper inside the disc.

In order to further constrain the origin of the emission lines, we show in Fig. 13, two diagnostic-diagrams: [N II]/Hα versus [O III]/Hβ (Baldwin, Phillips & Terlevich 1981), and $[S\,II]_{\lambda\lambda6717,6732}/H\alpha$ versus $[S\,III]_{\lambda\lambda9069,9532}/H\alpha$, which is particularly sensitive to shock-heating (Diaz, Pagel & Wilson 1985; Bonatto, Bica & Alloin 1989).

The two diagrams confirm the LINER classification for the nucleus. The top one suggests a similar classification for the locations 84 arcsec E and 52 arcsec E. The other extranuclear extractions are found in the loci corresponding to H II regions, consistent with the presence of a significant contribution of blue stellar components, as found in their continuum synthesis (Section 3.1). However, in the bottom diagram, all extranuclear spectra occupy the LINER loci.

We conclude that we are seeing a disc rich in H II regions, but with an important contribution from diffuse gas with emission characteristics similar to that in LINERs. The ionization mechanism in LINERs seems not to be unique – both shock ionization (Heckman 1980) and photoionization with a low ionization parameter can produce the observed line ratios (Ferland & Netzer 1983). In the present case, shock ionization could result from the interaction of a disc galaxy with the giant elliptical (Phillips 1981). Besides, in central regions of spiral galaxies a diffuse gas with shock emission characteristics is often observed (Storchi-Bergmann, Wilson & Baldwin 1995b; Storchi-Bergmann et al. 1996). However, some contribution from photoionization cannot be ruled out.

5 SUMMARY AND CONCLUDING REMARKS

In this paper we have investigated the origin of the continuum in the central 2.2 kpc of NGC 5128 through long-slit observations along the east–west direction running across the dusty disc.

We find that all the extracted spectra have a red stellar population component typical of a galactic bulge with varying contributions from a blue component. This latter contribution is absent outside the dust lane, has a maximum at intermediate distances in the dust lane, and decreases towards the centre. Simple syntheses show that this blue component is dominated by nuclear scattered light (power law) at the borders of the dusty disc, and for more internal regions throughout the disc, can be well represented by a blue stellar population template affected by different amounts of reddening, originating in regions of recent star formation located at different depths within the dust lane. However, we remark that, even for regions within the disc, a small contribution to this blue continuum from nuclear scattered light cannot be excluded.

From the population syntheses we find reddenings affecting the continua varying from $A_V = 0.0$ outside the dust lane up to $A_V = 3.6$ inside it, in agreement with results from imaging (Schreier et al. 1996). In most locations there is also an additional reddening intrinsic to the gas which can be as high as $A_V = 1.0$–3.0 mag.

The above results concerning variations of extinction, and the relative changes of stellar populations along the slit, bring out a picture of the dust and stellar components distribution throughout the disc. In particular, we suggest that the peaks of the young components at intermediate distances (extractions 30 arcsec W and 52 arcsec E from the nucleus) may result from spiral arms seen tangentially in the nearly edge-on disc.

The nucleus and locations 52 arcsec E and 84 arcsec E show emission line characteristics of a LINER. In the other locations, the optical line ratios are more typical of H II regions that are apparently embedded at different depths within the dusty disc. However, the near-infrared sulphur lines show that there is also some contribution from shocks, confirming evidences pointed out by other authors (e.g. Phillips 1981). Such shocks may have originated in the interaction of the disc with the elliptical galaxy or in diffuse gas in the disc, and could also be responsible for the LINER spectra of extractions 52 arcsec E and 84 arcsec E. Nevertheless, some contribution from photoionization cannot be discarded.

The comparison of the *IUE* and optical results for the nucleus shows that the ultraviolet is dominated by a moderately reddened ($A_V \approx 0.9$) disc component whereas at the near-infrared, a very reddened ($A_V \approx 3.0$) bulge population dominates. This means that at different wavelengths we are probing different depths and stellar population components. This makes NGC 5128 a very complex case for the derivation of an extragalactic reddening law, as was possible for starburst galaxy nuclei (Kinney et al. 1994; Calzetti, Kinney & Storchi-Bergmann 1994).

Finally, we would like to stress that we found in this paper evidence for the presence of young stellar populations in the nearest

© Royal Astronomical Society • Provided by the NASA Astrophysics Data System

Downloaded from http://mnras.oxfordjournals.org/ at FundaÃ§Ã£o CoordenaÃ§Ã£o de AperfeiÃ§oamento de Pessoal de NÃ-vel Superior on February 27, 2014

1997MNRAS.290..231S

radio galaxy Centaurus A, and demonstrated the importance of differential reddening when modelling integrated spectra of stellar populations affected by a dust lane. This result is particularly significant in the study of more distant radio galaxies, which show many similar features and for which the origin of the ultraviolet/optical continuum is still a matter of debate.

ACKNOWLEDGMENTS

TS-B, EB. and CB thank the Brazilian institutions CNPq, FINEP and FAPERGS for support. ALK would like to thank CNPq for support for a collaborative visit to the Instituto de Física da UFRGS, and the STScI Directors Discretionary Fund for support for this project. Finally, we would like to thank the referee for valuable suggestions which helped us to improve the paper. et al.

REFERENCES

Baldwin J. A., Phillips M. M., Terlevich R., 1981, PASP, 93, 5
Bica E., 1988, A&A, 195, 76
Bica E., Alloin D., 1986a, A&A, 162, 21
Bica E., Alloin D., 1986b, A&AS, 66, 171
Bica E., Alloin D., 1987, A&A, 186, 49
Bica E., Alloin D., Santos J. F., Jr, 1990, A&A, 235, 103
Bonatto C. J., Bica E., Alloin D., 1989, A&A, 226, 23
Bonatto C. J., Bica E., Pastoriza M. G., Alloin D., 1996, A&AS, 118, 89
Bouchet P., Lequex J., Maurice E., Prevot L., Prevot-Burnichon M. L., 1985, A&A, 149, 330
Brodie J., Königl A., Bowyer S., 1983, ApJ, 273, 154
Burns J. O., Feigelson E. D., Schreier E. J., 1983, ApJ, 273, 128
Calzetti D., Kinney A. L., Storchi-Bergmann T., 1994, ApJ, 429, 582
Chambers K. C., Miley G. K., van Breugel W., 1987, Nat, 329, 604
Diaz A. I., Pagel B., Wilson R., 1985, MNRAS, 212, 737
Feigelson E. D., Schreier E. J., Delvaille J. P., Giacconi R., Grindlay J. E., Lightman A. P., 1981, ApJ, 251, 31
Ferland G. J., Netzer H., 1983, ApJ, 264, 105
Giles A. B., 1986, MNRAS, 218, 615
Graham J. A., 1979, ApJ, 232, 60
Harris G. L. H., Geisler D., Harris H. C., Hesser J. E., 1992, AJ, 104, 613
Heckman T. M., 1980, A&A, 87, 152
Jablonka P., Bica E., Pelat D., Alloin D., 1996, A&A, 307, 385
Kinney A. L., Calzetti D., Bica E., Storchi-Bergmann T., 1994, ApJ, 429, 172
Kunkel W. E., Bradt H. V., 1971, ApJ, 170, L7
McCarthy P. J., 1993, ARA&A, 31, 639
McCarthy P. J., van Breugel W., Spinrad H., Djorgovski S., 1987, ApJ, 321, L29
McQuade K., Calzetti D., Kinney A. L., 1995, ApJS, 97, 331
Morganti R., Robinson A., Fosbury R. A. E., di Serego Alighieri S., Tadhunter C. N., Malin D. F., 1991, MNRAS, 249, 91
Osterbrock D. E., 1989, Astrophysics of Gaseous Nebulae and Active Galactic Nuclei. University Science Books, Mill Valley, California
Phillips M. M., 1981, MNRAS, 197, 659
Sandage A., Tammann G. A., 1981, in A Revised Shapley Ames Catalog of Bright Galaxies. Carnegie Institution of Washington Pub. 635
Schreier E. J., Capetti A., Macchetto F., Sparks W. B., Ford H. J., 1996, ApJ, 459, 535
Seaton M. J., 1979, MNRAS, 187, 73P
Sersic J. L., 1967, in Atlas de Galaxias Australes. Observatorio Astronomico, Cordoba, Argentina
Stone R. P. S., Baldwin J. A., 1983, MNRAS, 204, 347
Storchi-Bergmann T., Kinney A. L., Challis P., 1995a, ApJS, 98, 103
Storchi-Bergmann T., Wilson A. S., Baldwin J. A., 1995b, ApJ, 460, 252
Storchi-Bergmann T., Rodriguez-Ardila A., Schmitt H. R., Wilson A. S., Baldwin J. A., 1996, ApJ, 472, 83
Tadhunter C. N., Dickson R. C., Shaw N. A., 1996, MNRAS, 281, 591
Turner P., Forrest W. J., Pipher J. L., 1992, ApJ, 393, 648

This paper has been typeset from a TEX/LATEX file prepared by the author.

Downloaded from http://mnras.oxfordjournals.org/ at FundaÃ§Ã£o CoordenaÃ§Ã£o de AperfeiÃ§oamento de Pessoal de NÃ-vel Superior on February 27, 2014

© Royal Astronomical Society • Provided by the NASA Astrophysics Data System